*Title : will be set by the publisher*
*Editors : will be set by the publisher*
*EAS Publications Series, Vol. ?, 2012*

# A FAST METHOD FOR CONSTRUCTING MAGNETIC FIELD MODELS OF SOLAR ACTIVE REGIONS

I.V. Oreshina[1] and B.V. Somov[1]

**Abstract.** A new method is proposed for automatic choosing the so-called magnetic "charges" that are necessary to model the coronal magnetic field in solar ARs. The method makes the quantitative analysis of large-scale magnetic field fast, easy, and reliable that allows us to study the evolution of ARs on short time scales.

## 1 Introduction

It is well recognized that solar flares take their energy from the coronal magnetic field. However, the direct reliable and routine measurements of this field are not yet available. So we need magnetic field extrapolation methods to study the coronal field structure, topology and evolution.

One of the powerful tools to reconstruct coronal field is a magnetic charge model. It assumes that a real magnetic field can be modelled by that created by "effective charges". This approach allows us to distinguish different magnetic fluxes and the places where these fluxes interact among themselves, i.e. to study magnetic-field topology. Such models are developed since more than 20 years, see a review on this topic e.g. in Somov (2006).

It is possible to distinguish two main types of such models: the charges can be located either on the photospheric plane or under this plane. The models of the first type allows the quantitative estimations to be easy because exactly half of the flux from a charge enters the corona. However these models have singularities (charges) on the photosphere; moreover, the vertical component of magnetic field is zero everywhere on the photosphere except the points where charges are located. It makes impossible a comparison between an observed magnetogram and a model one (Barnes et al. 2005; Des Jardins et al. 2009; Kazachenko et al. 2010; Longcope et al.2010).

[1] Sternberg Astronomical Institute, Moscow State University, Russia; e-mail: ivo@sai.msu.ru & somov@sai.msu.ru


DOI: (will be inserted later)

The advantage of the models of the second type is the realistic approximation for the observed photospheric field and the shapes of EUV and X-ray flare ribbons (Gorbachev & Somov 1990; Mandrini et al. 1991; Démoulin et al. 1993; Somov et al. 2005; Oreshina & Somov 2008).

Automatic algorithms for choosing charges were proposed by Barnes *et al.*(2005) for the models from the first type and by Démoulin *et al.*(1994) for the case when charges are located under the photosphere at different depths. In our study we would like to join the advantages of both types: to make possible a quantitative analysis of magnetograms and to approximate the observed photospheric field well. We also want to make the model the most simple, the most clear in order to replace a 3D analysis by a 2D one when it is possible. So we propose an automatic algorithm for choosing the magnetic charges located under the photosphere in the same horizontal plane.

## 2 Method for choosing charges

Let the 3D magnetic field in the corona be described by formula

$$\mathbf{B}\,(x,y,z) = \sum_{i=1}^{N} \frac{e_i}{\mid \mathbf{r}-\mathbf{r}_i \mid^2} \cdot \frac{\mathbf{r}-\mathbf{r}_i}{\mid \mathbf{r}-\mathbf{r}_i \mid}\,,$$

where $N$ – number of charges, $\mathbf{r}_i = (x_i, y_i, z_i)$ – their radius vectors, $e_i$ – their intensities. The $x$-axis is directed to the west, the $y$-axis is directed to the north, and the $z$-axis is directed upward from the solar surface. Let us define the $z = 0$ plane as the photosphere. We locate all the charges under the photosphere at the same depth: $z_i = \text{const} = z_0$ for every $i$. So, there are $3N + 2$ unknowns: $(x_i, y_i)$, $e_i$ where $i = 1 \ldots N$, $z_0$, and $N$.

We propose the following algorithm to choose magnetic charges.

*STEP 1:* choosing the number of charges ($N$). The maximal absolute value of the photospheric field in a large solar flare is about 3000 G. Let us consider the areas where magnetic field value exceeds the 200 G level. This threshold allows us not to analyze the small-scale changes. We also neglect small areas covering a few pixels. So, we obtain $N$ areas $R_i$, $i = 1 \ldots N$ which determine the large-scale topology of an AR.

*STEP 2:* calculating charge positions $(x_i, y_i)$ as the "center of mass" of every area $R_i$:

$$x_i = \frac{\sum\limits_{k \in R_i} x_k \psi_k}{\sum\limits_{k \in R_i} \psi_k}\,, \qquad y_i = \frac{\sum\limits_{k \in R_i} y_k \psi_k}{\sum\limits_{k \in R_i} \psi_k}\,. \tag{2.1}$$

Here $\psi_k$ is the observed magnetic flux through the area on the photosphere that corresponds to the pixel $k$; $x_k$ and $y_k$ are the coordinates of this pixel. The summation is over all pixels forming the area $R_i$. Please note that we use the index $i$ to denote the summation over the charges and the index $k$ to denote the summation over the pixels within the area $R_i$.

*STEP 3:* finding charge intensities $e_i$ from the equality of the observed and the model magnetic fluxes for each area $R_i$:

$$\begin{cases} \sum\limits_{k\in R_1}\left[\sum\limits_{i=1}^{N}\dfrac{e_i}{|\mathbf{r}_k-\mathbf{r}_i|^2}\,\dfrac{(z_k-z_0)}{|\mathbf{r}_k-\mathbf{r}_i|}\right]\cdot s\;=\Psi_1; \\ \ldots \\ \sum\limits_{k\in R_N}\left[\sum\limits_{i=1}^{N}\dfrac{e_i}{|\mathbf{r}_k-\mathbf{r}_i|^2}\,\dfrac{(z_k-z_0)}{|\mathbf{r}_k-\mathbf{r}_i|}\right]\cdot s\;=\Psi_N. \end{cases} \tag{2.2}$$

Here $\Psi_i$ is the observed magnetic flux in the area $R_i$, $s$ the surface of a magnetogram pixel, $z_k$ the $z$-coordinate of pixel $k$. As we calculate the magnetic flux through the photosphere, $z_k = 0$.

There are $N$ equations with $N+1$ unknowns in this system: $e_1 \ldots e_N$ and $z_0$. We consider the value $z_0$ as a free parameter. Different values of $z_0$ will correspond to different sets of intensities $e_1 \ldots e_N$.

*STEP 4:* choosing the set which approximates the global magnetic flux in the best way:

$$\begin{cases} \sum\limits_{k_+}\left[\sum\limits_{i=1}^{N}\dfrac{e_i}{|\mathbf{r}_k-\mathbf{r}_i|^2}\,\dfrac{(z_k-z_0)}{|\mathbf{r}_k-\mathbf{r}_i|}\right]\cdot s\;-\Psi_+=\Delta_+; \\ \sum\limits_{k_-}\left[\sum\limits_{i=1}^{N}\dfrac{e_i}{|\mathbf{r}_k-\mathbf{r}_i|^2}\,\dfrac{(z_k-z_0)}{|\mathbf{r}_k-\mathbf{r}_i|}\right]\cdot s\;-\Psi_-=\Delta_-. \end{cases}$$

The summation in the first (second) formula is over all magnetogram pixels with positive (negative) magnetic field. $\Psi_+(\Psi_-)$ – observed positive (negative) magnetic fluxes in the whole AR.

In order to process other magnetograms of a same AR we keep the same depth $z_0$ and recalculate only the charges positions $(x_i, y_i)$ from formula 2.1 and their intensities from system 2.2.

## 3 Model of the AR NOAA 10501 on 2003 November 18

In this section we apply the method to study the evolution of NOAA AR 10501 between 00:00 UT and 11:12 UT on 2003 November 18. During this period, three flares occurred in this AR: C3.8 at 05:25 UT, M3.2 at 07:52 UT, and M3.9 at 08:30 UT. Two last flares were the most powerful and were associated with two CMEs (Srivastava et al. 2009; Chandra et al. 2010).

Figure 1 (left) presents the line-of-sight magnetogram obtained by MDI/SOHO at 00:00 UT. We show five largest areas where magnetic field was the most intense. Figure 1 (right) shows the result of modelling: vector magnetic field in the charge plane. The corresponding charge coordinates and intensities are presented in Table 1. Solid lines are the intersections of the separatrices with the plane $z_0$. As we see, there are four null points in this plane: $X_1$, $X_2$, $X_3$, and $X_4$. It is easy to show that there are two separators in this AR: the first one connects the points

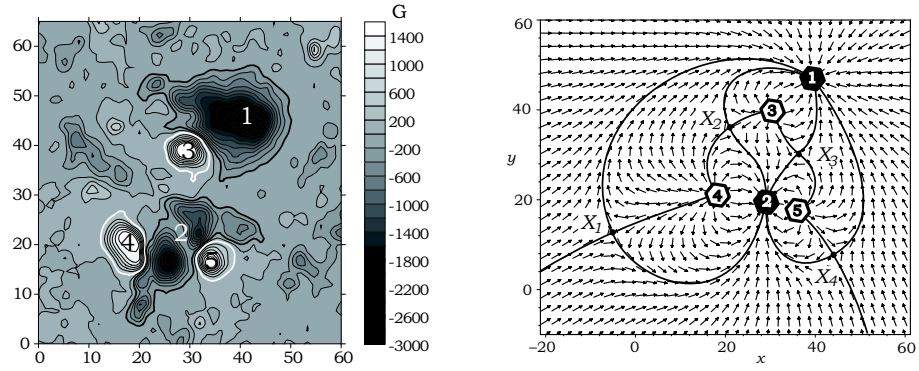


**Fig. 1.** *Left pannel:* Magnetogram obtained by MDI/SOHO at 00:00 UT on 2003 Nov 18. The white (black) thick lines are 200 G (-200 G) levels. A length unit corresponds to one MDI pixel ($1.45 \cdot 10^8$ cm). *Right pannel*: Magnetic vector field in the charge plane. Solid lines are the intersections of the separatrix surfaces with this plane. $X_1$, $X_2$, $X_3$, and $X_4$ are the null points.

$X_2$ and $X_3$ while the second one connects the points $X_3$ and $X_4$. *The observed flares can be explained by the magnetic reconnection on these separators.*

**Table 1.** Configuration of charges for modelling the magnetogram obtained at 00:00 UT.

| $i$ | $e_i$ | $x_i$ | $y_i$ | $z_0$ |
|---|---|---|---|---|
| 1. | -98317 | 39.5 | 46,9 | -4 |
| 2. | -79537 | 29.2 | 19.5 | -4 |
| 3. | 30834 | 30.4 | 39.6 | -4 |
| 4. | 36272 | 18.3 | 21.0 | -4 |
| 5. | 35496 | 35.7 | 17.8 | -4 |

Let us now consider a set of eight magnetograms obtained by MDI/SOHO with 96 min intervals, construct magnetic charge model for every magnetogram, find separators and calculate magnetic field strength on them. As it was demonstrated by Somov & Titov (1985), Somov (2006, Sect. 6.2.2), the weaker the longitudinal component of the magnetic field on a separator, the larger energy can be released in the reconnecting current layer. Fig. 2 presents the maximum values of magnetic field on both separators before and after the flares. Black circles correspond to the separator $X_2X_3$ and white circles correspond to the separator $X_3X_4$. We can see that *two most powerful flares (M class) occurred in the vicinity of the deepest magnetic field minimum on the separator* $X_3X_4$. It was also a minimum on the separator $X_2X_3$ even if not so deep.

More details about our method and the possible scenario of observed events in this AR can be found in Oreshina *et al.* (2012).

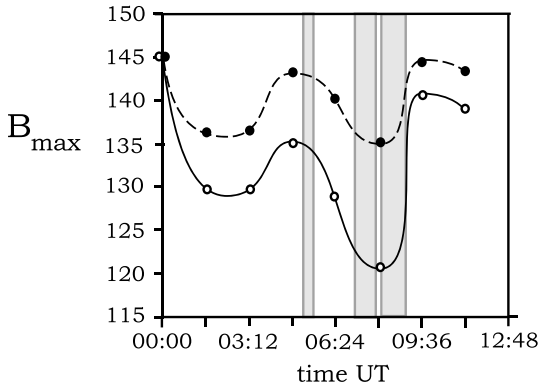


**Fig. 2.** Maximum values of magnetic field (in Gauss) on both separators: black circles correspond to the separator $X_2X_3$, white circles correspond to the separator $X_3X_4$. Three vertical gray strips show the times of three flares: C3.8 at 05:25 UT, M3.2 at 07:52 UT, and M3.9 at 08:30 UT.

## Acknowledgments

I.V. Oreshina is very grateful to the LOC for financial support and hospitality in Nice. We took the magnetograms from the web site http://soi.stanford.edu/data/ and we would like to thank the SOHO team for the availability of these data. This work was supported by the RFBR grant number 11-02-00843-a.

## References

Barnes, G. *et al.* 2005, ApJ, 629, 561

Chandra, R. *et al.* 2010, Solar Phys. 261, 127

Démoulin, P. *et al.* 1993, A&A, 271, 292

Démoulin, P. *et al.*1994, Solar Phys. 150, 221

Des Jardins, A. *et al.* 2009, ApJ, 693, 1628

Gorbachev, V. S. & Somov, B. V. 1990, Adv. Space Res., 10, Issue 9, 105

Kazachenko, M. D. *et al.* 2010, ApJ, 722, 1539

Longcope, D. W. *et al.* 2010, Solar Phys., 267, 107

Mandrini, C. H. *et al.* 1991, A&A, 250, 541

Oreshina, A. V. *et al.* 2012, A&A, (in press).

Oreshina, I. V. & Somov, B. V. 2008, Astron. Notes, 329, No. 8, 786

Somov, B. V. 2006, Plasma Astrophysics, Part II, Reconnection and Flares (New York: Springer Science + Business Media, LLC)

Somov, B. V. & Titov, V. S. 1985, Solar Phys. 102, No 1, 79

Somov, B. V. *et al.* 2005, Adv. Space Res., 35, 1712

Srivastava, N. *et al.* 2009, J. Geophys. Res. 114, Issue A3, CiteID A03107